Atmos. Chem. Phys. Discuss., 9, 11185–11220, 2009
www.atmos-chem-phys-discuss.net/9/11185/2009/

Atmospheric Chemistry and Physics Discussions

This discussion paper is/has been under review for the journal *Atmospheric Chemistry and Physics (ACP)*. Please refer to the corresponding final paper in *ACP* if available.

Quantifying atmospheric nitrate formation pathways based on a global model of the oxygen isotopic composition ($\Delta^{17}O$) of atmospheric nitrate

B. Alexander[1], M. G. Hastings[2], D. J. Allman[1], J. Dachs[3], J. A. Thornton[1], and S. A. Kunasek[4]

[1]Department of Atmospheric Sciences, University of Washington, Seattle, WA, USA
[2]Department of Geological Sciences and Environmental Change Initiative, Brown University, Providence, RI, USA
[3]Department of Environmental Chemistry, Instituto de Investigaciones Químicas y Ambientales de Barcelona/Consejo Superior de Investigaciones Científicas, Barcelona, Spain
[4]Department of Earth and Space Sciences, University of Washington, Seattle, WA, USA

Received: 15 April 2009 – Accepted: 24 April 2009 – Published: 5 May 2009

Correspondence to: B. Alexander (beckya@u.washington.edu)

Published by Copernicus Publications on behalf of the European Geosciences Union.

Abstract

The oxygen isotopic composition ($\Delta^{17}O$) of atmospheric nitrate is a function of the relative abundance of atmospheric oxidants (O_3, HO_x=OH+HO_2+RO_2) and the formation pathway of nitrate from its precursor NO_x(=NO+NO_2). Coupled observations and modeling of nitrate $\Delta^{17}O$ can be used to quantify the relative importance of chemical formation pathways leading to nitrate formation and reduce uncertainties in the budget of reactive nitrogen chemistry in the atmosphere. We present the first global model of atmospheric nitrate $\Delta^{17}O$ and compare with available observations. The model shows the best agreement with a global compilation of observations when assuming a $\Delta^{17}O$ value of tropospheric ozone equal to 35‰ and preferential oxidation of NO_x by the terminal oxygen atoms of ozone. Calculated values of annual-mean nitrate $\Delta^{17}O$ in the lowest model layer (0–200 m above the surface) vary from 6‰ in the tropics to 41‰ in the polar-regions. On the global scale, O_3 is the dominant oxidant (81% annual-mean) during NO_x cycling reactions. The global, annual-mean tropospheric inorganic nitrate burden is dominated by nitrate formation via NO_2+OH (76%), followed by N_2O_5 hydrolysis (18%) and NO_3+DMS/HC (4%). Model discrepancies are largest in the polar spring and summer, most likely due to the lack of reactive halogen chemistry in the model. The influence of organic nitrates on observations of nitrate $\Delta^{17}O$ needs to be determined, especially for observations in summertime and tropical forested regions where organic nitrates can contribute up to 80% of the total NO_y (organic plus inorganic nitrate) budget.

1 Introduction

The formation and cycling of reactive nitrogen in the atmosphere has important implications for air quality, the oxidation capacity of the atmosphere, and atmospheric nitrate (nutrient) deposition. Combustion of fossil fuels, biofuels, and biomass and lightning converts or "fixes" inert nitrogen gas (N_2) into a highly reactive form (NO_x=NO+NO_2).

ACPD

9, 11185–11220, 2009

Other sources of NO_x to the atmosphere include microbial processes in soils and transport from the stratosphere (Logan, 1983). Anthropogenic activities currently dominate NO_x sources to the troposphere (Jaegle et al., 2005). The influence of human activities on the atmospheric nitrogen budget is evident in the record of increasing nitrate concentrations over the past ~100 years in Greenland ice cores (Mayewski et al., 1990).

The photochemical cycling of NO_x leads to the formation of tropospheric ozone (O_3), a major air pollutant. Tropospheric ozone and its byproduct, the hydroxyl radical (OH), largely determine the oxidizing capacity of the atmosphere and the lifetime of most reduced trace gases (Thompson, 1992). The formation of nitrate, defined herein as gas-phase HNO_3 plus particulate NO_3^-, is the main sink of NO_x in the atmosphere. Nitrate is soluble and is lost from the atmosphere through wet and dry deposition to the Earth's surface, providing a nutrient source to many ecosystems (Galloway et al., 2008).

The oxygen isotopic composition of nitrate reflects the relative importance of different oxidants in NO_x cycling and nitrate formation (Michalski et al., 2003; Hastings et al., 2003). Understanding the importance of different oxidants for NO_x cycling and the pathways of nitrate formation is critical for understanding the budget of reactive nitrogen in the atmosphere. Here we present the first global chemical transport model of the oxygen isotopic composition of atmospheric nitrate. Comparison with available observations sheds light on previous assumptions used in box model studies regarding the isotopic composition of ozone and the isotopic transfer function during NO_x oxidation reactions, and provides a means to test and validate the model's representation of reactive nitrogen chemistry.

2 Controls on oxygen isotopic composition ($\Delta^{17}O$) of atmospheric nitrate

Atmospheric nitrate exhibits an anomalous ("mass-independent") oxygen isotopic composition. The isotopic composition of atmospheric nitrate is considered anomalous due to enrichment in ^{17}O relative to ^{18}O over the expected relationship ($\delta^{17}O \approx 0.5 \times \delta^{18}O$)

that results from purely mass-dependent fractionation processes (Matsuhisa et al., 1978). Isotope ratios are expressed in "delta notation",

$$\delta^x\mathrm{O}(‰) = \left[\frac{(\mathrm{O}^x/\mathrm{O}^{16})_{\mathrm{sample}}}{(\mathrm{O}^x/\mathrm{O}^{16})_{\mathrm{standard}}} - 1\right] \times 10^3 , \quad (1)$$

where x=17 or 18 and the standard used for oxygen isotopic analysis is Standard Mean Ocean Water (SMOW). The mass-independent oxygen isotopic anomaly in nitrate, quantified here as $\Delta^{17}\mathrm{O}=\delta^{17}\mathrm{O}-0.52\times\delta^{18}\mathrm{O}$, results mainly from the transfer of an isotopic anomaly in atmospheric ozone during oxidation of NO and NO_2 (R1 and R6 in Fig. 1).

Observations of the mean Δ^{17}O value of tropospheric ozone ($\Delta^{17}\mathrm{O}(\mathrm{O}_3)$) at different locations range from 25–35‰ (Johnston and Thiemens, 1997; Krankowsky et al., 1995). This large range in observed $\Delta^{17}\mathrm{O}(\mathrm{O}_3)$ is unexpected based on the pressure and temperature dependence of the isotopic enrichment measured in laboratory studies (Morton et al., 1990). This discrepancy may be due to a bias (most likely low) in the observational data from this difficult measurement and/or uncertainties in the laboratory data. A photochemical equilibrium model constrained with laboratory data (Janssen et al., 1999; Mauersberger et al., 1999) calculates Δ^{17}O=35‰ for surface ozone, increasing to 38‰ at the tropopause (Lyons, 2001). (Michalski and Bhattacharya, 2009) calculated $\Delta^{17}\mathrm{O}(\mathrm{O}_3)$=33–37‰ using a quadratic fit of data from (Morton et al., 1990) assuming temperatures and pressures typical of mid-latitudes. Other oxidants (OH, RO_2, HO_2) involved in NO_x cycling and nitrate formation have Δ^{17}O values at or near zero (Dubey et al., 1997; Savarino and Thiemens, 1999a; Lyons, 2001; Savarino and Thiemens, 1999b). Observations of the Δ^{17}O value of atmospheric nitrate (Δ^{17}O(nitrate)) range from ∼10–40‰ (Kaiser et al., 2007; McCabe et al., 2007; Michalski et al., 2003; Morin et al., 2007, 2008; Savarino et al., 2007; Brothers et al., 2008) highlighting the importance of ozone for reactive nitrogen chemistry in the atmosphere.

Reactive bromine (BrO) can also play a role in both NO_x cycling and nitrate formation in polar regions (Evans et al., 2003; Saiz-Lopez et al., 2008). BrO participates in NO_x cycling and nitrate formation through the following reactions:

$$NO + BrO \rightarrow NO_2 + Br \quad \text{(R9)}$$

$$NO_2 + BrO + M \rightarrow BrONO_2 + M \quad \text{(R10)}$$

$$BrONO_2 + H_2O_{(aq)} \rightarrow HOBr + HNO_3 \quad \text{(R11)}$$

BrO is expected to have $\Delta^{17}O$ values greater than $\Delta^{17}O(O_3)$ due to the involvement of O_3 in BrO formation and expected preferential oxidation of Br by the terminal oxygen atom of ozone (Morin et al., 2007). The formation of nitrate through BrO oxidation and $BrONO_2$ hydrolysis is expected to lead to similarly large $\Delta^{17}O$(nitrate) values (>40‰) (Morin et al., 2007). The global importance of reactive bromine in NO_x cycling and nitrate formation remains to be quantified.

3 Model description

We utilize the GEOS-Chem global 3-D model of coupled aerosol-oxidant chemistry (Park et al., 2004) to simulate nitrate $\Delta^{17}O$ observations. The model (version 8.01; see http://www-as.harvard.edu/chemistry/trop/geos/geos_versions.html) uses assimilated meteorological data from the NASA Goddard Earth Observing System (GEOS-4) including winds, convective mass fluxes, mixed layer depths, temperature, precipitation, and surface properties. Meteorological data have 6 h temporal resolution (3 h for surface variables and mixing depths). Meteorological fields have 1°×1° horizontal resolution with 48 sigma vertical levels (including seven below 1 km for a column based at sea-level). For input into GEOS-Chem, we degrade the horizontal resolution to 4°×5° and vertical resolution to 30 sigma levels. We conduct simulations for the year 2005 after a 12 month spin-up. The model was also run using May–June 2003 meteorological fields at 2°×2.5° horizontal resolution for comparison with the COCA cruise samples (see Sect. 4).

The tropospheric O_3-NO_x-hydrocarbon simulation was first described by (Bey et al., 2001) with updates by (Fiore et al., 2002; Martin et al., 2002). Emissions of NO_x total 39.3 Tg N yr^{-1} including sources from fossil fuel burning (including aircraft) (25.2 Tg N yr^{-1}), biofuel (2.2 Tg N yr^{-1}), biomass burning (5.3 Tg N yr^{-1}), lightning (0.1 Tg N yr^{-1}) and soil (including fertilizer) (6.6 Tg N yr^{-1}). Anthropogenic NO_x emissions were taken from the Global Emission Inventory Activity (GEIA) (Benkovitz et al., 1996), scaled by country on the basis of energy statistics to the year 1995 as described by (Bey et al., 2001). The monthly inventory of emissions from biomass burning are from the Global Fire Emissions Database (GFEDv2.1) for the year 2005 (Randerson et al., 2007; van der Werf et al., 2006). Soil NO_x emissions are computed using a modified version of the algorithm proposed by (Yienger and Levy, 1995) with the canopy reduction factors described by (Wang et al., 1998). Emissions of NO_x from lightning are linked to deep convection following the parameterization of (Price and Rind, 1992) with vertical profiles taken from (Pickering et al., 1998). Stratospheric NO_y (=NO_x+HNO_3) concentrations are calculated using NO_y production rates and its partitioning into NO_x and HNO_3 provided by a global 2-D stratospheric chemistry model (Schneider et al., 2000). The model transports stratospheric HNO_3 and NO_x into the troposphere; however, there no explicit representation of polar stratospheric cloud (PSC) sedimentation and resulting stratospheric denitrification.

Figure 1 summarizes the chemistry of NO_x cycling and nitrate formation in the atmosphere as simulated in the model. Upon emission, NO_x cycles rapidly during the daytime between NO and NO_2 via oxidation reactions (R1–R3) and photolysis (R4). NO is oxidized to NO_2 by ozone (O_3) (R1) and peroxy radicals (HO_2 and RO_2) (R2–R3). NO_2 is also produced through decomposition or oxidation of peroxyacyl nitrates (PANs), reactions of peroxy radicals (RO_2) with peroxynitrates (RO_2NO_2) and alkyl nitrates ($RONO_2$), and oxidation or decomposition of nitrous acid (HONO), pernitric acid (HNO_4), nitrate radicals (NO_3) and dinitrogen pentoxide (N_2O_5). NO_2 is lost from the atmosphere through oxidation and dry deposition to the surface. NO_2 is oxidized by OH (daytime) to form HNO_3 (R5) or by O_3 to form NO_3 (R6). NO_3 is rapidly photolyzed

during the daytime, so that NO_3 concentrations are only significant at night. At night, NO_3 reacts with dimethylsulfide (DMS) or hydrocarbons (HC) (R7) or with NO_2 to form N_2O_5 followed by hydrolysis on the surface of aerosols (R8) to form HNO_3. The lifetime of NO_x against conversion to HNO_3 in the boundary layer varies from ~1 day (tropics and in summer in the mid-to-high latitudes) to ~3 days (high latitudes in winter), similar to (Levy et al., 1999). Nitrate is lost from the atmosphere mainly through wet and dry deposition.

The aerosol and oxidant chemistry are coupled through the formation of sulfate and nitrate, heterogeneous chemistry, and aerosol effects on photolysis rates. Optical properties are calculated for each aerosol component as a function of local relative humidity as described by (Martin et al., 2003). Reactions involving aerosols are described by (Jacob, 2000) with updates for N_2O_5 hydrolysis as described in (Evans and Jacob, 2005). Photolysis frequencies are computed using the Fast-J radiative transfer algorithm (Wild et al., 2000) which allows for Raleigh scattering as well as for Mie scattering by clouds and aerosols. Total inorganic nitrate is partitioned between the gas and particulate (≤1 µm diameter) phases for the K^+-Ca^{2+}-Mg^{2+}-NH_4^+-Na^+-SO_4^{2-}-NO_3^--Cl^--H_2O aerosol system using the ISORROPIA II thermodynamic equilibrium model (Fountoukis et al., 2007). We also consider kinetic uptake of HNO_3 by coarse-mode sea-salt aerosol (>1 µm diameter) in competition with SO_2 as described in (Alexander et al., 2005). Wet deposition of aerosols is as described in (Liu et al., 2001) and includes contributions from scavenging in convective updrafts, rainout and washout from convective anvils and large-scale precipitation, and return to the atmosphere following re-evaporation. Dry deposition velocities for coarse-mode aerosols (>1 µm diameter) are computed with the size dependent scheme of (Zhang et al., 2001) integrated over each model size bin and accounting for hygroscopic growth as a function of relative humidity (Gerber, 1985). Dry deposition velocities for all other species are computed with a standard resistance-in-series scheme based on (Wesely, 1989) as described in (Wang et al., 1998).

Calculation of $\Delta^{17}O$(nitrate) in the model applies a mass transfer approach similar to

that first employed by (Michalski et al., 2003). During the daytime, reactions involving the photochemical cycling of NO and NO_2 (R1–R4) will achieve photochemical steady-state at least 3 orders of magnitude faster than conversion of NO_x to HNO_3 (R5–R8) (Sander et al., 2000; DeMore et al., 1997). Ignoring for now the potential influence of reactive bromine chemistry, the $\Delta^{17}O$ value of NO_x ($\Delta^{17}O(NO_x)$) is determined by the relative production rates of NO_2 via reaction of NO with O_3 (R1), HO_2 (R2) and RO_2 (R3) and the $\Delta^{17}O$ value of O_3,

$$\Delta^{17}O(NO_x)=A \times \Delta^{17}O(O_3) \tag{2a}$$

$$A = \frac{k_{R1}[NO][O_3]}{k_{R1}[NO][O_3] + k_{R2}[NO][HO_2] + k_{R3}[NO][RO_2]} \tag{2b}$$

where k_{R1}, k_{R2}, and k_{R3} represent rate constants for reactions R1, R2 and R3 respectively. The above calculation assumes that $\Delta^{17}O(HO_2)$=0‰, in contrast to observations of $\Delta^{17}O(H_2O_2)$ between 1–2‰ (H_2O_2 forms mainly through the self reaction of HO_2) (Savarino and Thiemens, 1999b). However, the assumption that $\Delta^{17}O(HO_2)$=0‰ versus $\Delta^{17}O(HO_2)$=2‰ changes our calculated $\Delta^{17}O$(nitrate) by less than 1‰ over the global range of calculated A values (Fig. 3 and Sect. 5.2) and simplifies the calculations. The assumption that $\Delta^{17}O(HO_2)$=0‰ is also consistent with other studies (Michalski et al., 2003; Morin et al., 2008; Kunasek et al., 2008). The ~1–3 day lifetime of NO_x against oxidation to HNO_3 suggests that NO_x will achieve isotopic equilibrium locally with O_3, HO_2, and RO_2 during the daytime prior to conversion to nitrate. The local $\Delta^{17}O(NO_x)$ is thus calculated in the model based on the relative NO_2 production rates (R1–R3) between 10:00–14:00 hours local time. Comparing calculated A values using NO_2 production rates averaged between 10:00–14:00 local time and 24 h has little impact on calculated $\Delta^{17}O$(nitrate) (generally <2‰) because of the strong diurnal cycling in NO_2 production rates.

Nitrate in the model is transported as four separate tracers depending on its production pathway (R5–R8 in Fig. 1 plus stratospheric nitrate). Each nitrate tracer is

assigned a $\Delta^{17}O$ value according to its involvement with O_3 during formation, similar to that proposed by (Michalski et al., 2003):

$$\Delta^{17}O(\text{nitrate})_{R5} = 2/3A\Delta^{17}O(O_3) \tag{3a}$$

$$\Delta^{17}O(\text{nitrate})_{R6,R7} = 2/3A\Delta^{17}O(O_3) + 1/3\Delta^{17}O(O_3) \tag{3b}$$

$$\Delta^{17}O(\text{nitrate})_{R6,R8} = 1/3A\Delta^{17}O(O_3) + 1/2\left(2/3A\Delta^{17}O(O_3) + 1/3\Delta^{17}O(O_3)\right) \tag{3c}$$

$$\Delta^{17}O(\text{nitrate})_{strat} = 5/6\Delta^{17}(O_3)_{strat} \tag{3d}$$

We assume O_3 will dominate NO_x cycling in the stratosphere leading to A=1. We use a factor of 5/6 to calculate the $\Delta^{17}O$ value of stratospheric nitrate ($\Delta^{17}O(\text{nitrate})_{strat}$) to be consistent with other studies (McCabe et al., 2007; Savarino et al., 2007) that assume stratospheric nitrate forms via N_2O_5 hydrolysis. This neglects nitrate formation via $ClONO_2$ decomposition and possible non-zero values of $\Delta^{17}O(H_2O)_{strat}$ (Franz et al., 2005; Zahn et al., 2006), leading to a possible underestimate of $\Delta^{17}O(\text{nitrate})_{strat}$. However, our results are insensitive to this assumption as stratospheric nitrate is a negligible source of nitrate in the model (Sect. 5.2).

$\Delta^{17}O(\text{nitrate})$ is calculated according to the local importance of O_3 in NO_x cycling (A) and the relative abundance of each nitrate tracer according to the following,

$$\Delta^{17}O(\text{nitrate}) = f_{R5}\Delta^{17}O(\text{nitrate})_{R5} + f_{R6,R7}\Delta^{17}O(\text{nitrate})_{R6,R7} + f_{R6,R8}\Delta^{17}O(\text{nitrate})_{R6,R8} + f_{strat}\Delta^{17}O(\text{nitrate})_{strat} \tag{4a}$$

$$f_{R5} = \frac{[\text{nitrate}]_{R5}}{[\text{nitrate}]_{total}}, f_{R6,R7} = \frac{[\text{nitrate}]_{R6,R7}}{[\text{nitrate}]_{total}}, f_{R6,R8} = \frac{[\text{nitrate}]_{R6,R8}}{[\text{nitrate}]_{total}}, f_{strat} = \frac{[\text{nitrate}]_{strat}}{[\text{nitrate}]_{total}} \tag{4b}$$

$$f_{R5} + f_{R6,R7} + f_{R6,R8} + f_{strat} = 1 \tag{4c}$$

where, for example, $[\text{nitrate}]_{R5}$ is the concentration of nitrate formed through NO_2+OH (R5), and $[\text{nitrate}]_{total}$ is the total concentration of inorganic nitrate. This formulation captures the effect of transport on $\Delta^{17}O(\text{nitrate})$ with respect to oxidation

of NO_2 to HNO_3. It does not capture the effect of transport on $\Delta^{17}O(NO_x)$ due to the use of local A values in calculating $\Delta^{17}O$(nitrate). This greatly simplifies the calculations but introduces some error in calculated values of $\Delta^{17}O$(nitrate). This error will be most significant in remote regions with no local sources of NO_x (e.g. polar winter) – the magnitude of this error (maximum of 5‰) is explored in more detail in Sect. 5.3.

We perform sensitivity studies to cover the range of observed tropospheric $\Delta^{17}O(O_3)$ values (25–35‰) and differing assumptions for the transfer mechanism of the isotopic anomaly from O_3 to NO_2 and NO_3 upon oxidation (R1 and R6). We assume stratospheric $\Delta^{17}O(O_3)$=40‰ in all simulations, a value towards the upper end of observations (10.4–45.7‰) (Mauersberger et al., 2001) and consistent with model studies (Liang et al., 2006). Previous box-model studies have assumed either an equal likelihood of all three O-atoms of O_3 (Michalski et al., 2003; Kunasek et al., 2008) or favored oxidation by the terminal O-atom of O_3 (Morin et al., 2008) during oxidation of NO and NO_2. Whether or not the terminal O-atom of ozone is favored as the reacting atom influences the resulting isotopic composition of nitrate because the asymmetric isotopologues of ozone are enriched in heavy oxygen isotopes with respect to bulk ozone (e.g. $^{18}O^{16}O^{16}O$ vs. $^{16}O^{18}O^{16}O$) (Janssen, 2005; Bhattacharya et al., 2008; Michalski and Bhattacharya, 2009). Recent laboratory experiments suggest that the isotopic transfer of the terminal O-atom of ozone is favored during oxidation of NO to NO_2 according to $\Delta^{17}O(NO_x)_{R1}=1.18\pm0.07\times\Delta^{17}O(O_3)+6.6\pm1.5$ (Savarino et al., 2008).

4 Observations

The observations include monthly average $\Delta^{17}O$(nitrate) of aerosol samples collected from Alert, Canada (82° N, 85° W) (Morin et al., 2008), La Jolla, California (33° N, 117° W) (Michalski et al., 2003), Dumont D'Urville, Antarctica (66° S, 140° E) (Savarino et al., 2007), and the South Pole (McCabe et al., 2007). Event-based rainwater samples are averaged over each month of collection from Princeton, New Jersey (40° N,

75° W) (Kaiser et al., 2007) and Bermuda (32° N, 65° W) (Hastings et al., 2003) to compare with monthly-resolved model output. Fog-water samples collected in the Podocarpus National Forest, Ecuador (4° S, 79° W) are averaged over the course of three years (2004–2006) (Brothers et al., 2008). The observations also include seasonally-resolved snowpit samples from Summit, Greenland (73° N, 39° W) (Kunasek et al., 2008), and annual-average nitrate collected from passive deposition collectors in the Atacama desert (Yungay), Chile (24° S, 70° W) (Ewing et al., 2007).

Daily-averaged aerosol samples collected during the COCA cruise in the subtropical north Atlantic in May–June 2003 (21–28° N, 14–26° W) aboard the RV *Hespérides* (Dachs et al., 2005; Duarte et al., 2006) are presented here for the first time (see supplementary material for details http://www.atmos-chem-phys-discuss.net/9/11185/2009/acpd-9-11185-2009-supplement.pdf). Aerosol samples were collected on quartz fiber filters (QFF, Whatmann, pre-combusted at 450°C for 8 h) with a high-volume aerosol sampler for ~24 h per sample and shipped to the University of Washington for concentration (NO_3^-) and isotopic ($\Delta^{17}O$(nitrate)) analysis. Filters were sonnicated in 18 MΩ water, filtered, and measured for NO_3^- concentration via ion chromatography. Measured concentrations of NO_3^- (0.2–8.3 μg m^{-3}) were used to determine if there was enough sample for isotopic analysis (~6 μmol of nitrate), and samples were combined as necessary for a total of 16 isotopic measurements. For each sample, organics were removed (oxidized) by adding an excess of a 30% (by volume) H_2O_2 solution and then analysis of $\Delta^{17}O$(nitrate) was performed according to methods outlined in (Kunasek et al., 2008). Briefly, the NO_3^- was isolated from each sample by anion separation using an ion chromatograph and converted to $AgNO_3$ using a cation exchange membrane. Each $AgNO_3$ sample was then dried in a silver capsule, and pyrolyzed at 550°C to form O_2+NO_2 (+NO, N_2 in trace amounts) in continuous-flow mode using a Finnigan Thermocouple Elemental Analyzer (TC/EA) interfaced with a Finnigan MAT 253 Isotope Ratio Mass Spectrometer (IRMS) with He as the carrier gas. NO_2 and other byproducts of $AgNO_3$ pyrolysis are removed at liquid nitrogen temperature, and O_2 is measured for $^{16}O^{16}O$, $^{16}O^{17}O$ and $^{16}O^{18}O$ from which $\Delta^{17}O$ is calculated. Our measurements

of the USGS-35 reference material ($NaNO_3$) produce $\Delta^{17}O$(nitrate)=21.6±0.3(1σ) for sample sizes ranging from 5–7 µmol NO_3^-, which agrees with the accepted value of 21.6‰ (Bohlke et al., 2003).

Observations of $\Delta^{17}O$(nitrate) were made using two types of analysis: the "silver salt pyrolysis" method (Michalski et al., 2002) described above (observations from La Jolla, South Pole, Summit, Chile, Ecuador and COCA) and the "denitrifier" method (Kaiser et al., 2007) (observations from Alert, Dumont D'Urville, Princeton, Bermuda). The silver salt pyrolysis method relies on isolation of dissolved, inorganic nitrate (NO_3^-) prior to analysis. Nitrate anion separation ensures that only inorganic nitrate is measured, assuming that soluble organic nitrate does not dissociate in water. Observations of C_1–C_5 alkyl nitrates in wet deposition (rain, snow, frost) (Hauff et al., 1998) suggest that they do not readily dissociate. The denitrifier method does not require isolation of NO_3^- and uses denitrifying bacteria (*Pseudomonas aureofaciens*) to convert nitrate (and nitrite) into N_2O, which is then quantitatively thermally decomposed into O_2 and N_2. The O_2 isotopes are then measured on-line using an IRMS. It is generally assumed that the denitrifier method selectively measures inorganic nitrate; however, this has yet to be specifically demonstrated. As will be shown, whether or not we include organic nitrates in our isotope calculations is significant for calculated $\Delta^{17}O$(nitrate) in regions where organic nitrates are abundant.

5 Results and discussion

5.1 Model comparison with observations

Figure 2 compares $\Delta^{17}O$(nitrate) model results with observations. The model is sampled at the same time resolution as the observations (daily, monthly and annual mean). Each panel represents a different assumption in the model regarding the isotopic composition of ozone and the isotopic transfer mechanism. Assuming $\Delta^{17}O(O_3)$=35‰ with a statistical transfer during O_3 oxidation of NO and NO_2 (Fig. 2a), or assuming

$\Delta^{17}O(O_3)$=25‰ with the empirical $\Delta^{17}O$ isotopic transfer function of (Savarino et al., 2008) during the $NO+O_3$ reaction (Fig. 2c), results in an underestimate of $\Delta^{17}O$(nitrate) observations at all locations by as much as 45% (equivalent to a 15‰ underestimate of $\Delta^{17}O$(nitrate)). Using $\Delta^{17}O(O_3)$=35‰ with the (Savarino et al., 2008) transfer during $NO+O_3$ only (Fig. 2b) and during both the $NO+O_3$ and NO_2+O_3 reactions (Fig. 2d) reduces the low bias, and in general agrees with observations within 25% (equivalent to agreement of $\Delta^{17}O$(nitrate) within 10‰).

Based on Fig. 2, we focus our analysis using the latter model simulation that assumes $\Delta^{17}O(O_3)$=35‰ with the (Savarino et al., 2008) $\Delta^{17}O$ transfer applied to both the $NO+O_3$ and NO_2+O_3 reactions. Although the comparison in Fig. 2 suggests that $\Delta^{17}O(O_3)$=35‰ is the appropriate value to use in calculations of $\Delta^{17}O$(nitrate), it is no substitute for direct observations of $\Delta^{17}O(O_3)$, as model biases will impact our results. For example, if the true $\Delta^{17}O(O_3)$=25‰, then our finding that $\Delta^{17}O(O_3)$=35‰ provides the best agreement between observed and modeled $\Delta^{17}O$(nitrate) indicates that the model globally and systematically underestimates (overestimates) O_3 and/or NO_3 (OH and/or peroxy radical) concentrations. The resulting magnitude of the bias in $\Delta^{17}O$(nitrate) will be dependent upon the magnitude of bias in O_3, NO_3, OH, or peroxy radical concentrations. Our calculated global mean OH concentration (10.7×10^5 molecules cm^{-3}) compares well with (Wang et al., 2008) (10.6×10^5 molecules cm^{-3}) who optimized the global abundance of OH by interpreting observations of methyl chloroform using an inverse technique and the GEOS-Chem model. This suggests no global, systematic bias in OH. Calculated O_3 concentrations in the GEOS-Chem model has been extensively evaluated against observations (Wang et al., 2009; Hudman et al., 2009; Zhang et al., 2008; Terao et al., 2008; Wu et al., 2007), suggesting no systematic global bias. Peroxy radical concentrations would have to be overestimated globally by a factor of ~3 to account for a 10‰ difference in $\Delta^{17}O(NO_x)$. Although we may expect significant regional biases in these radical concentrations, a systematic global bias seems unlikely for species with a high degree of

spatial variability.

5.2 Global variability of tropospheric nitrate formation pathways and Δ^{17}O(nitrate)

Figure 3 shows global plots of modeled summer (JJA) and winter (DJF) mean Δ^{17}O(nitrate) and the local fraction of NO oxidized to NO_2 via O_3 (A) at the in the lowest model layer (0–200 m above the surface). Δ^{17}O(nitrate) ranges from 6–41‰ with A ranging from 0.16–1.00. The spatial variability of Δ^{17}O(nitrate) is largely determined by the importance of O_3 in NO_x cycling (A) due to the fact that the isotopic composition of two-thirds of the oxygen atoms of nitrate is determined during NO_x cycling. The oxidation of NO_x to nitrate plays a secondary but significant role in determining the final Δ^{17}O(nitrate) value.

Figure 4 shows the fractional importance of each nitrate production pathway to annual mean nitrate concentrations in the lowest model layer (0–200 m above the surface). Nitrate production via NO_2+OH (R5) dominates (up to 87%) in the tropics where OH concentrations are highest. Nitrate production via N_2O_5 hydrolysis (R8) dominates (up to 74%) at high northern latitudes over the continents and the Arctic, consistent with observations and modeling by (Tie et al., 2003) and (Stroud et al., 2003). Nitrate production via reaction of NO_3 with (primarily) DMS (R7) is most important (up to 46%) in the high latitudes in the marine boundary layer. The stratospheric source of nitrate is negligible (annual average maximum of 2% in Antarctica). The annual-mean fractional contribution to the tropospheric inorganic nitrate burden for nitrate formed via NO_2+OH (R5), N_2O_5 hydrolysis (R6, R8), and NO_3+DMS/HC (R6,R7) is 76%, 18%, and 4%, respectively. The remaining inorganic nitrate burden (2%) is from the stratosphere.

The largest values of Δ^{17}O(nitrate) occur in the winter hemisphere high latitudes (Fig. 3) due to the increased importance of O_3 in NO_x cycling (R1) and nitrate formation (R6). (McCabe et al., 2007) estimated an annual average contribution of 25% stratospheric nitrate at the South Pole to explain their high (38.1‰) late-winter val-

ues of $\Delta^{17}O$(nitrate). In their analysis, (McCabe et al., 2007) assumed tropospheric $\Delta^{17}O(O_3)$=27.1±4.8‰ and an isotopic transfer mechanism that results in a depletion of $\Delta^{17}O$(nitrate) relative to $\Delta^{17}O(O_3)$. In contrast, our calculated winter (July) $\Delta^{17}O$(nitrate) at the South Pole (39.6‰) is similar in magnitude to the observations (McCabe et al., 2007), with stratospheric nitrate contributing <5% in winter. It is important to note here that we are likely underestimating the stratospheric source in polar-regions due to the lack of an explicit stratospheric denitrification mechanism from the sedimentation of PSCs in the model. Indeed, stratospheric nitrate is thought to be an important (but unquantified) source of nitrate to Antarctica (Legrand and Kirchner, 1990; McMorrow et al., 2004; Mulvaney and Wolff, 1993; Wagenbach et al., 1998; Weller et al., 2002; Savarino et al., 2007). However our results suggest that $\Delta^{17}O$(nitrate) values on the order of 40‰ can be explained by a dominant source of tropospheric nitrate.

The smallest values of $\Delta^{17}O$(nitrate) occur in the summer hemisphere and in the tropics due to the increased importance of peroxy radicals (R2 and R3) in NO_x cycling and nitrate production via NO_2+OH (R5), with annual mean values as low as 6‰ in tropical forested regions. Observations (using the silver salt pyrolysis method) of $\Delta^{17}O$(nitrate) in fog-water collected in the Podocarpus National Forest, Ecuador (4° S, 79° W) show a range of annual average values over three years (2004–2006) of 13–22‰ (Brothers et al., 2008). Our monthly-mean model results vary between 14–20‰ with an annual-average of 17‰ at this location.

5.3 Model discrepancies

Figure 5 compares monthly-mean $\Delta^{17}O$(nitrate) model calculations with observations available over the course of a full year (Alert, Summit, Princeton, La Jolla, DDU, and the South Pole). The model reproduces the seasonality of the $\Delta^{17}O$(nitrate) observations. The model shows good agreement (generally within 3‰) with the observations in low- to mid-latitudes (La Jolla, Bermuda, COCA, Chile and Ecuador; Fig. 2), though additional observations in low-latitude forested regions are necessary to validate model

predictions of Δ^{17}O(nitrate) less than 20‰. In general, the largest discrepancies occur during spring and summer in polar-regions (1–10‰ underestimate) and in the northern hemisphere mid- to high-latitudes (2–7‰ overestimate, maximum in winter).

The model underestimate (1–10‰) of Δ^{17}O(nitrate) maximizes in polar regions in spring when nitrate formation from $BrONO_2$ hydrolysis is expected to be significant (Morin et al., 2007; Evans et al., 2003; Saiz-Lopez et al., 2008). Bromine radical concentrations can be as high as ~30 ppt during spring in both the Arctic and Antarctic close to sea-ice (Chance, 1998;Richter et al., 1997; Wagner and Platt, 1998; Kreher et al., 1997). Several indirect lines of evidence suggest a non-negligible contribution of bromine radical chemistry in the inland Arctic (Summit, Greenland) during summer months (Grannas et al., 2007; Peterson and Honrath, 2001; Sjostedt et al., 2007), and are supported by BrO observations of 1–3 ppt during early summer at Summit, Greenland (Huey et al., 2007). The model underestimate of Δ^{17}O(nitrate) in the polar-regions during spring is likely due to the lack of BrO chemistry in the model, which may also contribute to the underestimate in summer. (Kunasek et al., 2008) estimated a 4‰ increase in summertime Δ^{17}O(nitrate) at Summit, Greenland after adding reactive bromine chemistry to their box model assuming BrO concentrations of 3 ppt. This suggests that BrO chemistry can fully account for the 4‰ underestimate in calculated Δ^{17}O(nitrate) at Summit in July (Fig. 5). In addition, photochemical processing of snowpack nitrate during spring and summer leads to a significant local source of NO_x in the polar-regions (Jones et al., 2000; Honrath et al., 2002) that is not accounted for in the model. Local reprocessing of previously deposited nitrate during periods of active bromine radical chemistry will enhance the importance of bromine in NO_x cycling and nitrate formation in the polar-regions.

Non-zero Δ^{17}O(OH) values due to incomplete exchange of OH with water vapor in the cold, dry polar atmosphere (Morin et al., 2007) may also contribute to the underestimate of Δ^{17}O(nitrate) in winter and spring. (Kunasek et al., 2008) estimated that ~10% of the original Δ^{17}O(OH) could be retained at Summit, Greenland in spring and summer. This would lead to a maximum underestimate of 1–2‰ in calculated Δ^{17}O(nitrate)

and may partially explain the spring/summer discrepancy in polar regions.

The model tends to overestimate $\Delta^{17}O$(nitrate) (2–7‰) in the northern mid-to high latitudes in winter when N_2O_5 hydrolysis dominates nitrate production (Fig. 4), suggesting that the model may be overestimating this nitrate production pathway. The reaction probability of N_2O_5 ($\gamma_{N_2O_5}$) on the surface of aerosols is influenced by temperature, humidity, and aerosol composition (Kane et al., 2001; Hallquist et al., 2003; Thornton et al., 2003). (Davis et al., 2008) suggested that $\gamma_{N_2O_5}$ may be overestimated by (Evans and Jacob, 2005) (used in GEOS-Chem), especially in regions of relatively low temperatures and high relative humidity. In addition, the presence of aerosol surface coating by organics has been shown to decrease $\gamma_{N_2O_5}$ (McNeill et al., 2006) and is not accounted for in the model. We examine the sensitivity of $\Delta^{17}O$(nitrate) to N_2O_5 hydrolysis by setting the reaction probability of N_2O_5 equal to zero ($\gamma_{N_2O_5}$=0), effectively shutting off this nitrate formation pathway. This increases $\Delta^{17}O$(nitrate), particularly at high latitudes during winter (Fig. 5), due to relative increases in both NO_2+OH (R5) and NO_3+DMS/HC (R7) nitrate formation pathways, with the latter reaction (R7) becoming more important. Removing N_2O_5 hydrolysis results in a 30% increase in the global, annual-mean tropospheric NOX (=NO_2+NO_3+HNO_2+2N_2O_5+HNO_4) burden. This effect of N_2O_5 hydrolysis on reactive nitrogen partitioning and loss is consistent with, but somewhat smaller than that found by an earlier analysis (50%) (Dentener and Crutzen, 1993), likely due to the different $\gamma_{N_2O_5}$ values used.

The model overestimates $\Delta^{17}O$(nitrate) at Princeton, NJ year round (2–7‰ in summer and winter, respectively). The Princeton data set represents event-based rainwater samples averaged over each month of collection and thus may not adequately represent the monthly-mean state. The Princeton observations may also be influenced by the presence of soluble organic nitrates, which are not included in the model calculations.

In light of the fact that the denitrifier method may be measuring a combination of organic and inorganic nitrates, we examine the potential influence of soluble organic

nitrates by including them in our isotope calculations. Soluble organic nitrates included in our isotope calculations form in the model mainly from reactions of $NO+RO_2$ to form isoprene nitrates ($RONO_2$), where RO_2 in this case originates from isoprene oxidation products. Soluble organic nitrates also form to a minor extent from reactions between isoprene nitrates (formed via isoprene+NO_3) and RO_2 (methylperoxy and peroxyacetyl radicals). Isoprene is a biogenic hydrocarbon whose main source is terrestrial vegetation, with emissions largely dependent upon vegetation type and density, light and temperature (Guenther et al., 1995). We use the Model of Emissions from Gases and Aerosols in Nature (MEGAN) to compute process-based biogenic emissions of isoprene and other trace gases (Guenther et al., 2006) as described in (Palmer et al., 2006; Millet et al., 2008). The model does not include soluble organic nitrates formed via oxidation of anthropogenic hydrocarbons in the presence of NO_x, which would most impact the formation of organic nitrates during winter when emission rates for biogenic hydrocarbons are low. The model treats soluble organic nitrates in a similar manner to inorganic nitrate, partitioning the organic nitrates between the gas and aerosol-phase according to thermodynamic equilibrium of HNO_3. Organic nitrates are then dry or wet deposited. The formation of organic nitrates is most important in regions where isoprene emissions are highest (forested regions in the low- to mid-latutides, maximum in summer).

The $\Delta^{17}O$ value of organic nitrates is calculated according to the following, for reactions with $NO+RO_2$ and isoprene nitrates+RO_2, respectively:

$$\Delta^{17}O(RONO_2)_{NO+RO_2} = 1/3A\Delta^{17}O(O_3) \quad (5a)$$

$$\Delta^{17}O(RONO_2)_{NO_3+RO_2} = 2/3A\Delta^{17}O(O_3) \quad (5b)$$

For the latter reaction, we assume that the organic nitrate retains two of the original oxygen atoms of NO_3, which may be an underestimate. However, our results are not particularly sensitive to this assumption since organic nitrates formed via this reaction pathway are a minor source of total (inorganic plus organic) nitrate (<6% annual mean). Organic nitrates formed via the $NO+RO_2$ pathway dominate (80% annual mean) total

nitrate in tropical forested regions, and are as high as 20% (annual mean) elsewhere. Model results that include organic plus inorganic nitrate in calculations of Δ^{17}O(nitrate) are shown in Fig. 5 for the observations that utilized the denitrifier method. Including organic nitrates derived from isoprene oxidation lowers the calculated Δ^{17}O(nitrate) values by as much as 3‰ at a mid-latitude continental location (Princeton, NJ) during summer, and as much as 10‰ in tropical forested regions.

The overestimate of Δ^{17}O(nitrate) in the polar winter (generally between 2–7‰) can be explained by the use of local *A* values in calculating Δ^{17}O(nitrate) where there is a negligible local source of NO_x and most of the nitrate originates from lower latitudes. The importance of ozone in NO_x cycling shows strong latitudinal dependence resulting in *A* values increasing with latitude (maximum in polar winter) (Fig. 3). The overestimate of Δ^{17}O(nitrate) due to the use of local *A* values is most pronounced in remote polar-regions in winter where nitrate originates from lower latitudes and local NO_x production (e.g. snowpack photodenitrification) is absent. An overestimate of the *A* value by 0.2 (typical difference between *A* values at 90° S and 45° S), leads to an overestimate of Δ^{17}O(nitrate) by 5‰, which is within the range of the overestimate in polar winter.

The difference between polar versus mid-latitude *A* values does not explain the maximum overestimate of Δ^{17}O(nitrate) (up to 13‰ in late autumn/early winter) at DDU, Antarctica (66° S latitude). (Savarino et al., 2007) attribute their measured low Δ^{17}O(nitrate) values (22–33‰) to nitrate originating at mid-latitudes, as the range in measured Δ^{17}O(nitrate) during austral summer and fall is similar to observations in Lolla, CA (33° N, 117° W) (Michalski et al., 2003). DDU contains a significant penguin population which could provide a biogenic source of organic nitrogen. Indeed, (Savarino et al., 2007) occasionally found penguin feathers and feces on their filter samples. If photolytic or thermal decomposition of organic nitrogen to inorganic nitrate occurred on the filters post collection (Zhang and Anastasio, 2003), this biogenic source of nitrogen would lower the measured Δ^{17}O(nitrate). However, penguin populations peak during summer, which is inconsistent with the seasonality of the under-

estimate (Savarino et al., 2007). Wagenbach et al. (1998) estimated negligible nitrate contamination from penguin colonies at this site.

6 Conclusions

We use the global 3-D chemical transport model, GEOS-Chem, to simulate the oxygen isotopic composition ($\Delta^{17}O$) of atmospheric nitrate and compare with available observations. These comparisons allow for quantitative assessment of the relative importance of different oxidants in NO_x cycling and nitrate formation pathways, and are critical for interpreting ice core observations of $\Delta^{17}O$(nitrate) in terms of changes in past oxidant concentrations (Alexander et al., 2004).

The largest uncertainty for calculations of $\Delta^{17}O$(nitrate) is the unconstrained variability in tropospheric $\Delta^{17}O(O_3)$. The best agreement with global observations occurs when assuming a $\Delta^{17}O(O_3)$=35‰ and using the (Savarino et al., 2008) isotopic transfer function during the reaction of O_3 with NO and NO_2. The spatial variability of $\Delta^{17}O$(nitrate) is largely determined by the importance of O_3 in NO_x cycling due to the fact that the isotopic composition of two-thirds of the oxygen atoms of nitrate is determined during NO_x cycling. The annual mean fractional contribution of O_3 in NO_x cycling (A) in the lowest model layer (0–200 m above the surface) ranges from 0.16 in the tropics to 1.00 in polar-regions. The oxidation pathway of NO_x to HNO_3 plays a secondary but significant role in determining $\Delta^{17}O$(nitrate) values. The global, annual-mean tropospheric inorganic nitrate burden (0.38 Tg N) is dominated by nitrate formation via NO_2+OH (76%), followed by N_2O_5 hydrolysis (18%) and NO_3+DMS/HC (4%).

Calculated values of annual-mean $\Delta^{17}O$(nitrate) in the lowest model layer (0–200 m above the surface) vary from 6‰ in the tropics to 41‰ in polar regions. Modeled annual-mean $\Delta^{17}O$(nitrate) values greater than 40‰ exist in the polar regions with negligible contribution from stratospheric nitrate (<2%). Modeled annual-mean

Δ^{17}O(nitrate) values as low as 6‰ are predicted in tropical forested regions due to the dominance of peroxy radicals and OH in NO_x cycling and nitrate formation, respectively. Additional measurements of Δ^{17}O(nitrate) in the tropics are needed to validate these results.

The largest model discrepancies are in polar-regions during spring and summer (1–10‰ underestimate), and in mid- to high latitudes in winter (general 2–7‰ overestimate). The former is likely due to the lack of reactive bromine chemistry in the model, which should peak in spring in polar regions and lead to large (>40‰) Δ^{17}O(nitrate) (Morin et al., 2007). The high bias in polar winter is due to the use of the local fractional importance of O_3 (versus HO_2+RO_2) in NO_x cycling (*A* value) for calculations of Δ^{17}O(nitrate) in regions where nitrate originates from lower latitudes. This overestimate is particularly pronounced in winter when local NO_x production (e.g., snowpack photodenitrification) is negligible. The high bias in the mid- to high-northern latitudes is amplified when removing nitrate formation via N_2O_5 hydrolysis in the model due to a relative increase in nitrate formation via nitrate radical H-abstraction reactions. The role (or lack thereof) of organic nitrates in observations of Δ^{17}O(nitrate) that utilize the denitrifier method (Kaiser et al., 2007; Casciotti et al., 2002) needs to be assessed. Whether or not organic nitrates are included in the calculation of Δ^{17}O(nitrate) has a significant impact in low- to mid-latitude continental regions, and may partially account for the high bias in the mid-latitude Δ^{17}O(nitrate) values.

Acknowledgements. We gratefully acknowledge funding of the COCA cruise by the Spanish Ministry of Science and Innovation, and financial support for this project from the NSF Atmospheric Chemistry Program under grant NSF-ATM 0607846 to B. Alexander. M. G. Hastings acknowledges partial support from the Joint Institute for the Study of the Atmosphere and Ocean (JISAO) under NOAA cooperative agreement No. NA17RJ1232 (contribution #XXXX). We thank D. Hegg and A. Schauer for assistance with nitrate concentration and isotopic measurements, respectively, for the COCA samples, and Lauren Brothers for sharing her data from Ecuador.

References

Alexander, B., Savarino, J., Kreutz, K. J., and Thiemens, M. H.: Impact of preindustrial biomass-burning emissions on the oxidation pathways of tropospheric sulfur and nitrogen, J. Geophys. Res., 109, D08303, doi:10.1029/2003JD004218, 2004.

Alexander, B., Savarino, J., Lee, C. C. W., Park, R. J., Jacob, D. J., Li, Q., Yantosca, R. M., and Thiemens, M. H.: Sulfate formation in sea-salt aerosols: Constraints from oxygen isotopes, J. Geophys. Res., 110, D10307, doi:10.1029/2004JD005659, 2005.

Benkovitz, C. M., Schultz, M. T., Pacyna, J., Tarrason, L., Dignon, J., Voldner, E. C., Spiro, P. A., Logan, J. A., and Graedel, T. E.: Global, gridded inventories for anthropogenic emissions of sulfur and nitrogen, J. Geophys. Res., 101, 29239–29253, 1996.

Bey, I., Jacob, D. J., Yantosca, R. M., Logan, J. A., Field, B. D., Fiore, A. M., Li, Q., Liu, H. Y., Mickley, L. J., and Schultz, M. G.: Global modeling of tropospheric chemistry with assimilated meteorology: Model description and evaluation, J. Geophys. Res., 106, 23073–23095, 2001.

Bhattacharya, S. K., Pandey, A., and Savarino, J.: Determination of intramolecular isotope distribution of ozone by oxidation reaction with silver metal, J. Geophys. Res., 113, D03303, doi:10.1029/2006JF008309, 2008.

Bohlke, J. K., Mroczkowski, S. J., and Coplen, T. B.: Oxygen isotopes in nitrate: new reference materials for O-18:O-17:O-16 measurements and observations on nitrate-water equilibration, Rapid Commun. Mass. Sp., 17, 1835–1846, 2003.

Brothers, L. A., Dominguez, G., Fabian, P., and Thiemens, M. H.: Using multi-isotope tracer methods to understand the sources of nitrate in aerosols, fog and river water in Podocarpus National Forest, Ecuador, Eos Trans. AGU, 89, Abstract A11C-0136, 2008.

Casciotti, K. L., Sigman, D. M., Hastings, M. G., Bohlke, K. K., and Hilkert, A.: Measurement of the oxygen isotopic composition of nitrate in seawater and freshwater using the denitrifier method, Anal. Chem., 74, 4905–4912, 2002.

Chance, K.: Analysis of BrO Measurements from the global ozone monitoring experiment, Geophys. Res. Lett., 25, 3335–3338, 1998.

Dachs, J., Calleja, M. L., Duarte, C. M., Vento, S. D., Turpin, B., Polisori, A., Herndl, G. J., and Agusti, S.: High atmosphere-ocean exchange of organic carbon in the NE subtropical Atlantic, Geophys. Res. Lett., 32, L21807, doi:10.1029/2005GL023799, 2005.

Davis, J. M., Bhave, P. V., and Foley, K. M.: Parameterization of N_2O_5 reaction probabilities on the surface of particles containing ammonium, sulfate, and nitrate, Atmos. Chem. Phys., 8,

5295–5311, 2008,
http://www.atmos-chem-phys.net/8/5295/2008/.
DeMore, B. W., Sander, S. P., Golden, D. M., Hampson, R. F., Kurylo, M. J., Howard, C. J., Ravishankara, A. R., Kolb, C. E., and Molina, M. J.: Chemical kinetics and photochemical data for use in stratospheric modeling, JPL Publ., 97-4, 1–278, 1997.
Dentener, F. J. and Crutzen, P. J.: Reaction of N_2O_5 on tropospheric aerosols: Impact on the global distributions of NO_x, O_3, and OH, J. Geophys. Res., 98, 7149–7163, 1993.
Duarte, C. M., Dachs, J., Llabres, M., Alonso-Laita, P., Gasol, J. M., Tovar-Sanchez, A., Sanudo-Wilhemy, S., and Agusti, S.: Aerosol inputs enhance new production in the subtropical northeast Atlantic, J. Geophys. Res., 111, G04006, doi:10.1029/2005JG000140, 2006.
Dubey, M. K., Mohrschladt, R., Donahue, N. M., and Anderson, J. G.: Isotope-specific kinetics of hydroxyl radical (OH) with water (H_2O): Testing models of reactivity and atmospheric fractionation, J. Phys. Chem. A., 101, 1494–1500, 1997.
Evans, M. J., Jacob, D. J., Atlas, E., Cantrell, C. A., Eisele, F., Flocke, F., Fried, A., Mauldin, R. L., Ridley, B. A., Wert, B., Talbot, R., Blake, D., Heikes, B., Snow, J., Walega, J., Weinheimer, A. J., and Dibb, J.: Coupled evolution of BrO_x-ClO_x-HO_x-NO_x chemistry during bromine-catalyzed ozone depletion events in the arctic boundary layer, J. Geophys. Res., 108, 8368, doi:10.1029/2002JD002732, 2003.
Evans, M. J. and Jacob, D. J.: Impact of new laboratory studies of N_2O_5 hydrolysis on global model budgets of tropospheric nitrogen oxides, ozone, and OH, Geophys. Res. Lett., 32, L09813, doi:10.1029/2005GL022469, 2005.
Ewing S. A., Michalski, G., Thiemens, M., Quinn, R. C., Macalady, J. L., Kohl, S., Wankel, S. D., Kendall, C., McKay, C. P., and Amundson R.: Rainfall limit of the N cycle on Earth, Global Biogeochem. Cy., 21, GB3009, doi:10.1029/2006GB002838, 2007.
Fiore, A. M., Jacob, D. J., Bey, I., Yantosca, R. M., Field, B. D., and Wilkinson, J. G.: Background ozone over the United States in summer: Origin and contribution to pollution episodes, J. Geophys. Res., 107, 4275, doi:10.1029/2001JD000982, 2002.
Fountoukis, C. and Nenes, A.: ISORROPIA II: a computationally efficient thermodynamic equilibrium model for K^+-Ca^{2+}-Mg^{2+}-NH_4^+-Na^+-SO_4^{2-}-NO_3^--Cl^--H_2O aerosols, Atmos. Chem. Phys., 7, 4639–4659, 2007,
http://www.atmos-chem-phys.net/7/4639/2007/.
Franz, P. and Röckmann, T.: High-precision isotope measurements of $H_2^{16}O$, $H_2^{17}O$, $H_2^{18}O$, and the $\Delta^{17}O$-anomaly of water vapor in the southern lowermost stratosphere, Atmos. Chem.

Phys., 5, 2949–2959, 2005, http://www.atmos-chem-phys.net/5/2949/2005/.

Galloway, N. J., Townsend, R. A., Erisman, W. J., Bekunda, M., Cai, Z., Freney, R. J., Martinelli, L. A., Seitzinger, S. P., and Sutton, M. A.: Transformation of the nitrogen cycle: Recent trends, questions, and potential solutions, Science, 320, 889–892, doi:10.1126/science.1136674, 2008.

Gerber, H. E.: Relative-humidity paramaterization of the Nave aerosol model (NAM), Natl. Res. Lab., Washington, D.C., 1985.

Grannas, A. M., Jones, A. E., Dibb, J., Ammann, M., Anastasio, C., Beine, H. J., Bergin, M., Bottenheim, J., Boxe, C. S., Carver, G., Chen, G., Crawford, J. H., Dominé, F., Frey, M. M., Guzmán, M. I., Heard, D. E., Helmig, D., Hoffmann, M. R., Honrath, R. E., Huey, L. G., Hutterli, M., Jacobi, H. W., Klán, P., Lefer, B., McConnell, J., Plane, J., Sander, R., Savarino, J., Shepson, P. B., Simpson, W. R., Sodeau, J. R., von Glasow, R., Weller, R., Wolff, E. W., and Zhu, T.: An overview of snow photochemistry: evidence, mechanisms and impacts, Atmos. Chem. Phys., 7, 4329–4373, 2007, http://www.atmos-chem-phys.net/7/4329/2007/.

Guenther, A., Hewitt, N. C., Erickson, D., Fall, R., Geron, C., Graedel, T., Harley, P., Klinger, L., Lerdau, M., McKay, W. A., Pierce, T., Scholes, B., Steinbrecher, R., Tallamraju, R., Taylor, J., Zimmerman, P.: A global model of natural volatile organic compound emissions, J. Geophys. Res., 100, 8873–8892, 1995.

Guenther, A., Karl, T., Harley, P., Wiedinmyer, C., Palmer, P. I., and Geron, C.: Estimates of global terrestrial isoprene emissions using MEGAN (Model of Emissions of Gases and Aerosols from Nature), Atmos. Chem. Phys., 6, 3181–3210, 2006, http://www.atmos-chem-phys.net/6/3181/2006/.

Hallquist, M., Stewart, D. J., Stephenson, S. K., and Cox, R. A.: Hydrolysis of N_2O_5 on submicron sulfate aerosol, Phys. Chem. Chem. Phys., 5, 3453–3463, 2003.

Hastings, M. G. and Sigman, D. M.: Isotopic evidence for source changes of nitrate in rain at Bermuda, J. Geophys. Res., 108(D24), 4790, doi:10.1029/2003JD003789, 2003.

Hauff, K., Fischer, R. G., and Ballschmiter, K.: Determination of C1-C5 alkyl nitrates in rain, snow, white frost, lake, and tap water by a combined codistillation head-space gas chromatography technique. Determination of henry's law constants by head-space GC, Chemosphere, 37, 2599–2615, 1998.

Honrath, E. R., Lu, Y., Peterson, C. M., Dibb, E. J., Arsenault, A. M., Cullen, J. N., and Steffen,

K.: Vertical fluxes of NO_x, HONO, and HNO_3 above the snowpack at Summit, Greenland, Atmos. Environ., 36, 2629–2640, 2002.

Hudman, R. C., Murray, L. T., Jacob, D. J., Turquety, S., Wu, S., Millet, D. B., Avery, M., Goldstein, A. H., and Holloway, J.: North American influence on tropospheric ozone and the effects of recent emission reductions: Constraints from ICARTT observations, J. Geophys. Res, 114, D07302, doi:10.1029/2008JD010126, 2009.

Huey, L. G., Dibb, J., Stutz, J., Brooks, S., von Glasow, R., Lefer, B., Chen, G., Kim, S., and Tanner, D.: Observations of halogens at Summit, Greenland, EOS Transactions, AGU, 88, Fall Meet. Suppl., Abstract A42B-05, 2007.

Jacob, D. J.: Heterogeneous chemistry and tropospheric ozone, Atmos. Env., 34, 2131–2159, 2000.

Jaegle, L., Steinberger, L., Martin, R. V., and Chance, K.: GLobal partitioning of NO_x sources using satellite observations: Relative roles of fossil fuel combustion, biomass burning and soil emissions, Faraday Discuss., 130, 407–423, doi:10.1039/b502128f, 2005.

Janssen, C., Guenther, J., and Krankowsky, D.: Relative formation rates of $^{50}O_3$ and $^{52}O_3$ in $^{16}O^-$ ^{18}O mixtures, J. Chem. Phys., 111, 7179–7182, 1999.

Janssen, C.: Intramolecular isotope distribution in heavy ozone ($^{16}O\,^{18}O\,^{16}O$ and $^{16}O\,^{16}O\,^{18}O$), J. Geophys. Res, 110, D08308, doi:10.1029/2004JD005479, 2005.

Johnston, J. C. and Thiemens, M. H.: The isotopic composition of tropospheric ozone in three environments, J. Geophys. Res., 102, 25395–25404, 1997.

Jones, A. E., Weller, R., Wolff, E. W., and Jacobi, A. H.-W.: Speciation and rate of photochemical NO and NO_2 production in Antarctic snow, Geophys. Res. Lett., 27, 345–348, 2000.

Kaiser, J., Hastings, M. G., Houlton, B. Z., Rockmann, T., and Sigman, D. M.: Triple Oxygen Isotope Analysis of Nitrate Using the Denitrifier Method and Thermal Decomposition of N_2O, Anal. Chem., 79, 599–607, 2007.

Kane, S. M., Caloz, F., and Leu, M. T.: Heterogeneous uptake of gaseous N_2O_5 by $(NH_4)_2SO_4$, NH_4HSO_4 and H_2SO_4 aerosol, J. Phys. Chem., 105, 6465–6570, 2001.

Krankowsky, D., Bartecki, F., Klees, G. G., Mauersberger, K., Schellenback, K., and Stehr, J.: Measurement of heavy isotope enrichment in tropospheric ozone, Geophys. Res. Lett., 22, 1713–1716, 1995.

Kreher, K., Johnson, P. V., Wood, S. W., Nardi, B., and Platt, U.: Ground-based measurements of tropspheric and stratospheric BrO at Arrivals Heights, Antarctica, Geophys. Res. Lett., 24, 3021–3024, 1997.

Kunasek, A. S., Alexander, B., Hastings, M. G., Steig, E. J., Gleason, D. J., and Jarvis, J. C.: Measurements and modeling of $\Delta^{17}O$ of nitrate in a snowpit from Summit, Greenland, J. Geophys. Res., 113, D24302, doi:10.1029/2008JD010103, 2008.

Legrand, M. R. and Kirchner, S.: Origins and variations of nitrate in south polar precipitation, J. Geophys. Res, 95, 3493–3507, 1990.

Levy, H., Moxim, W. J., Klonecki, A. A., and Kasibhatla, P. S.: Simulated tropospheric NO_x: Its evaluation, global distribution and individual source contributions, J. Geophys. Res., 104, 26279–26306, 1999.

Liang, M.-C., Irion, F. W., Weibel, J. D., Miller, C. E., Blake, G. A., and Yung, Y. L.: Isotopic composition of stratospheric ozone, J. Geophys. Res., 111, D02302, doi:10.1029/2005JD006342, 2006.

Liu, H., Jacob, D. J., Bey, I., and Yantosca, R. M.: Constraints from ^{210}Pb and ^{7}Be on wet deposition and transport in a global three-dimensional chemical tracer model driven by assimilated meterological fields, J. Geophys. Res., 106, 12109–12128, 2001.

Logan, J. A.: Nitrogen oxides in the troposphere: Global and regional budgets, J. Geophys. Res.-Oc. Atm., 88, 785–807, 1983.

Lyons, J. R.: Transfer of mass-independent fractioation on ozone to other oxygen-containing molecules in the atmosphere, Geophys. Res. Lett., 28, 3231–3234, 2001.

Martin, R. V., Jacob, D. J., Loganand, J. A., et al.: Interpretation of TOMS observations of tropical tropspheric ozone with a global model and in-situ observations, J. Geophys. Res., 107, 4351, doi:10.1029/2001JD001480, 2002.

Martin, R. V., Jacob, D. J., Yantosca, R. M., Chin, M., and Ginoux, P.: Global and regional decreases in tropospheric oxidants form photochemical effects of aerosols, J. Geophys. Res., 108, 4097, doi:4010.1029/2002JD002622, 2003.

Matsuhisa, Y., Goldsmith, J. R., and Clayton, R. N.: Mechanisms of hydrothermal crystallization of quartz at 250°C and 15 kbar, Geochim. Cosmochim. Acta, 42, 173–182, 1978.

Mauersberger, K., Erbacher, B., Krankowsky, D., Gunther, J., and Nickel, R.: Ozone isotope enrichment: Isotopomer-specific rate coefficients, Science, 283, 370–372, 1999.

Mauersberger, K., Lämmerzahl, P., and Krankowsky, D.: Stratospheric ozone isotope enrichments–revisited, Geophys. Res. Lett., 28, 3155–3158, 2001.

Mayewski, P. A., Lyons, W. B., Spencer, M. J., Twickler, M. S., Buck, C. F., and Whitlow, S.: An ice-core record of atmospheric response to anthropogenic sulphate and nitrate, Nature, 346, 554–556, 1990.

McCabe, J. R., Thiemens, M. H., and Savarino, J.: A record of ozone variability in South Pole Antarctic snow: Role of nitrate oxygen isotopes, J. Geophys. Res, 112, D12303, doi:10.1029/2006JD007822, 2007.

McMorrow, A., Ommen, T. D. V., Morgan, V., and Curran, M. A. J.: Ultra-high-resolution seasonality of trace-ion species and oxygen isotope ratios in Antarctic firn over four annual cycles, Ann. Glaciology, 39, 34–40, 2004.

McNeill, V. F., Patterson, J., Wolfe, G. M., and Thornton, J.: The Effect of Varying levels of Surfactant on the Reactive Uptake of N_2O_5 to Submicron Aqueous Aerosol, Atmos. Chem. Phys., 6, 1635–1644, 2006, http://www.atmos-chem-phys.net/6/1635/2006/.

Michalski, G. M., Savarino, J., Bohlke, J. K., and Thiemens, M. H.: Determination of the total oxygen isotopic composition of nitrate and the calibration of a $\Delta^{17}O$ nitrate reference material, Anal. Chem., 74, 4989–4993, 2002.

Michalski, G. M., Scott, Z., Kabiling, M., and Thiemens, M. H.: First measurements and modeling of $\Delta^{17}O$ in atmospheric nitrate, Geophys. Res. Lett., 30, 1870, doi:1810.1029/2003GL017015, 2003.

Michalski, G. and Bhattacharya, S. K.: The role of symmetry in the mass independent isotope effect in ozone, Proc. Natl. Acad. Sci., 106, 5493–5496, 2009.

Millet, D. B., Jacob, D. J., Boersma, K. F., Fu, T.-M., Kurosu, T. P., Chance, K., Heald, C. L., and Guenther, A.: Spatial distribution of isoprene emissions from North America derived from formaldehyde column measurements by the OMI satellite sensor, J. Geophys. Res., 113(D2), D02307, doi:10.1029/2007JD008950, 2008.

Morin, S., Savarino, J., Bekki, S., Gong, S., and Bottenheim, J. W.: Signature of Arctic surface ozone depletion events in the isotope anomaly ($\Delta^{17}O$) of atmospheric nitrate, Atmos. Chem. Phys., 7, 1451–1469, 2007, http://www.atmos-chem-phys.net/7/1451/2007/.

Morin, S., Savarino, J., Frey, M. M., Yan, N., Bekki, S., Bottenheim, J. W., and Martins, J. M. F.: Tracing the Origin and Fate of NO_x in the Arctic Atmosphere Using Stable Isotopes in Nitrate, Science, 322, 730–732, doi:10.1126/science.1161910, 2008.

Morton, J., Barnes, J., Schueler, B., and Mauersberger, K.: Laboratory studies of heavy ozone, J. Geophys. Res., 95, 901–907, 1990.

Mulvaney, R. and Wolff, E. W.: Evidence for winter/spring denitrification of the stratosphere in the nitrate record of antarctic firn cores, J. Geophys. Res., 98, 5213–5220, 1993.

Palmer, P. I., Abbot, D. S., Fu, T.-Z., Jacob, D. J., Chance, K., Kuruso, T. P., Guenther, A., Wiedinmyer, C., Stanton, J. C., Pilling, M. J., Pressley, S. N., Lamb, B., and Sumner, A. L.: Quantifying the seasonal and interannual variability of North American isoprene emissions using satellite observations of formaldehyde column, J. Geophys. Res., 111(D12), D12315, doi:10.1029/2005JD006689, 2006.

Park, R. J., Jacob, D. J., Field, B. D., Yantosca, R. M., and Chin, M.: Natural and transboundary pollution influences on sulfate-nitrate-ammonium aerosols in the United States: implications for policy, J. Geophys. Res., 109, D15204, doi:10.1029/2003JD004473, 2004.

Peterson, M. C. and Honrath, R. E.: Observations of Rapid Photochemical Destruction of Ozone in Snowpack Interstitial Air, Geophys. Res. Lett., 28, 511–514, 2001.

Pickering, K. E., Wang, Y. S., Tao, W. K., Price, C., and Muller, J. F.: Vertical distributions of lightning NO_x for use in regional and global chemical transport models, J. Geophys. Res, 103, 31203–231216, 1998.

Price, C. and Rind, D.: A simple lightning parameterization for calculating global lightning distribution, J. Geophys. Res., 97, 9919–9933, 1992.

Global Fire EMissions Database, Version 2 (GFEDv2.1). Data set. Available on line., 2007.

Richter, A., Wittrock, F., Eisinger, M., and Burrows, J. P.: GOME observations of tropospheric BrO in northern hemispheric spring and summer 1997, Geophys. Res. Lett., 25, 2683–2686, 1997.

Saiz-Lopez, A., Plane, J. M. C., Mahajan, A. S., Anderson, P. S., Barguitte, S. J.-B., Jones, A. E., Roscoe, H. K., Salmon, R. A., Bloss, W. J., Lee, J. D., and Heard, D. E.: On the vertical distribution of boundary layer halogens over coastal Antarctica: implications for O_3, HO_x, NO_x and the Hg lifetime, Atmos. Chem. Phys., 8, 887–900, 2008, http://www.atmos-chem-phys.net/8/887/2008/.

Sander, S. P., Friedl, R. R., Ravishankara, A. R., Golden, D. M., Kolb, C. E., Kurylo, M. J., Huie, R. E., Orkin, V. L., Molina, M. J., Moortgat, G. K., and Finlayson-Pitts, B. J.: Chemical Kinetics and Photochemical Data for use in Atmospheric Studies, NASA Jet Propulsion Lab, 2–25, 2000.

Savarino, J., Kaiser, J., Morin, S., Sigman, D. M., and Thiemens, M. H.: Nitrogen and oxygen isotopic constraints on the origin of atmospheric nitrate in coastal Antarctica, Atmos. Chem. Phys., 7, 1925–1945, 2007, http://www.atmos-chem-phys.net/7/1925/2007/.

Savarino, J. and Thiemens, M. H.: Mass-independent oxygen isotope (^{16}O, ^{17}O, ^{18}O) fraction-

ation found in H_x, O_x reactions, J. Phys. Chem., 103, 9221–9229, 1999a.
Savarino, J. and Thiemens, M. H.: Analytical procedure to determine both $\delta^{18}O$ and $\delta^{17}O$ of H_2O_2 in natural water and first measurements, Atmos. Env., 33, 3683–3690, 1999b.
Savarino, J., Bhattacharya, S. K., Morin, S., Baroni, M., and Doussin, J.-F.: The NO+O_3 reaction: A triple oxygen isotope perspective on the reaction dynamics and atmospheric implications for the transfer of the ozone isotope anomaly, J. Chem. Phys., 128, 2008.
Schneider, H. R., Jones, D. B. A., McElroy, M. B., and Shi, G.-Y.: Analysis of residual mean transport in the stratosphere 1. Model description and comparison with satellite data, J. Geophys. Res., 105, 19991–20011, 2000.
Sjostedt, S. J., Huey, L. G., Tanner, D. J., Peischl, J., Chen, G., Dibb, J. E., Lefer, B., Hutterli, M. A., Beyersdorf, A. J., Blake, N. J., Blake, D. R., Sueper, D., Ryerson, T., Burkhart, J., and Stohl, A.: Observations of hydroxyl and the sum of peroxy radicals at Summit, Greenland during summer 2003, Atmos. Env., 41, 5122–5137, 2007.
Stroud, C., Madronich, S., Atlas, E., Ridley, B., Flocke, F., Weinheimer, A., Talbot, B., Fried, A., Wert, B., Shetter, R., Lefer, B., Coffey, M., Heikes, B., and Blake, D.: Photochemistry in the arctic free troposphere: NO_x budget and the role of odd nitrogen reservoir recycling, Atmos. Env., 37, 3351–3364, 2003.
Terao, Y., Logan, J. A., Douglass, A. R., and Stolarski, R. S.: Contribution of stratospheric ozone to the interannual variability of tropospheric ozone in the northern extratropics, J. Geophys. Res, 113, D18309, doi:10.1029/2008JD009854, 2008.
Thompson, A. M.: The oxidizing capacity of the earth's atmosphere: Probable past and future changes, Science, 256, 1157–1165, 1992.
Thornton, J. A., Braban, C. F., and Abbatt, J. P. D.: N_2O_5 hydrolysis on sub-micron organic aerosol: The effect of relative humidity, particle phase and particle size, Phys. Chem. Chem. Phys., 5, 4593–4603, 2003.
Tie, X., Emmons, L., Horowitz, L., Brasseur, G., Ridley, B., Atlas, E., Stround, C., Hess, P., Klonecki, A., Madronich, S., Talbot, R., and Dibb, J.: Effect of sulfate aerosol on tropospheric NO_x and ozone budgets: Model simulations and TOPSE evidence, J. Geophys. Res, 108, 8364, doi:/10.1029/2001JD001508, 2003.
van der Werf, G. R., Randerson, J. T., Giglio, L., Collatz, G. H., and Kasibhatla, P. S.: Interannual variability in global biomass burning emission from 1997 to 2004, Atmos. Chem. Phys., 6, 3423–3411, 2006, http://www.atmos-chem-phys.net/6/3423/2006/.

Wagenbach, D., Legrand, M., Fischer, H., Pichlmayer, F., and Wolff, E. W.: Atmospheric near-surface nitrate at coastal Antarctic sites, J. Geophys. Res., 103, 11007–11020, 1998.
Wagner, T. and Platt, U.: Satellite mapping of enhanced BrO concentrations in the troposphere, Nature, 395, 486–490, 1998.
Wang, Y. H., Jacob, D. J., and Logan, J. A.: Global simulation of tropospheric O_3-NO_x hydrocarbon chemistry 1. Model formulation, J. Geophys. Res., 103, 10713–710725, 1998.
Wang, H., Jacob, D. J., Sager, P. L., Streets, D. G., Park, R. J., Gilliland, A. B., and Donkelaar, A. V.: Surface ozone background in the United States: Canadian and Mexican pollution influences, Atmos. Environ., in press, 2009.
Wang, J. S., McElroy, M. B., Logan, J. A., Palmer, P. I., Chameides, W. L., Wang, Y., and Megretskaia, I. A.: A quantitative assessment of uncertainties affecting estimates of global mean OH derived from methyl chloroform observations, J. Geophys. Res, 113, D12302, doi:10.1029/2007JD008496, 2008.
Weller, R., Jones, A. E., Wille, A., Jacobi, H.-W., McIntyre, H. P., Sturges, W. T., Huke, M., and Wagenbach, D.: Seasonality of reactive nitrogen oxides (NO_y) at Neumayer Station, Antarctica, J. Geophys. Res, 107, 4673, doi:10.1029/2002JD002495, 2002.
Wesely, M. L.: Parameterization of surface resistances to gaseous dry deposition in regional-scale numerical-models, Atmos. Env., 23, 1293–1304, 1989.
Wild, O., Zhu, Q., and Prather, M. J.: Fast-J: Accurate simulation of in- and below-cloud photolysis in global chemical models, J. Atm. Chem., 37, 245–282, 2000.
Wu, S., Mickley, L. J., Jacob, D. J., Logan, J. A., Yantosca, R. M., and Rind, D.: Why are there large differences between models in global budgets of tropospheric ozone?, J. Geophys. Res., 112, D05302, doi:10.1029/2006JD007801, 2007.
Yienger, J. J. and Levy, H.: Empirical model of global soil-biogenic NO_x emissions, J. Geophys. Res., 100, 11447–11464, 1995.
Zahn, A., Franz, P., Bechtel, C., Groob, J.-U., and Röckmann, T.: Modelling the budget of middle atmospheric water vapour isotopes, Atmos. Chem. Phys., 6, 2073–2090, 2006, http://www.atmos-chem-phys.net/6/2073/2006/.
Zhang, L., Gong, S., Padro, J., and Barrie, L.: A size-segregated particle dry deposition scheme for an atmosopheric aerosol module, Atmos. Env., 35, 549–560, 2001.
Zhang, L., Jacob, D. J., Boersma, K. F., Jaffe, D. A., Olson, J. R., Bowman, K. W., Worden, J. R., Thompson, A. M., Avery, M. A., Cohen, R. C., Dibb, J. E., Flock, F. M., Fuelberg, H. E., Huey, L. G., McMillan, W. W., Singh, H. B., and Weinheimer, A. J.: Transpacific transport of ozone

pollution and the effect of recent Asian emission increases on air quality on Notrh America: an integrated analysis using satellite, aircraft, ozonesonde, and surface observations, Atmos. Chem. Phys., 8, 6117–6136, 2008, http://www.atmos-chem-phys.net/8/6117/2008/.

Zhang, Q. and Anastasio, C.: Conversion of fogwater and aerosol organic nitrogen to ammonium, nitrate, and NO_x during exposure to simulated sunlight and ozone, Environ. Sci. Technol., 37, 3522–3530, doi:10.1021/es034114x, 2003.

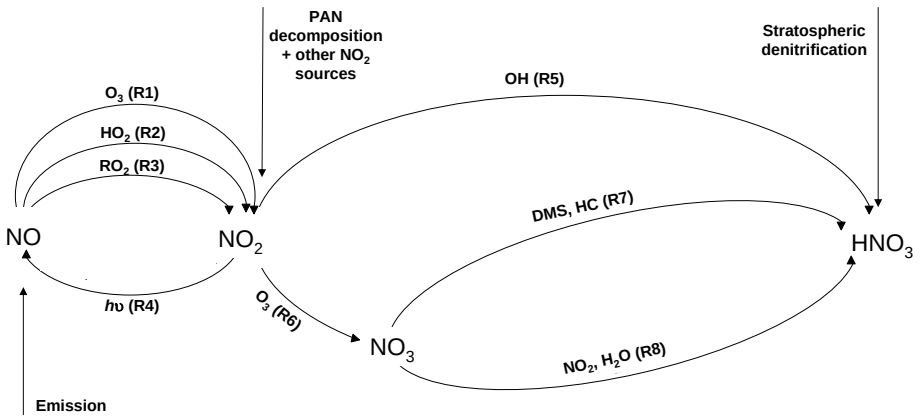

Fig. 1. Simplified chemistry leading to inorganic nitrate formation in the model.

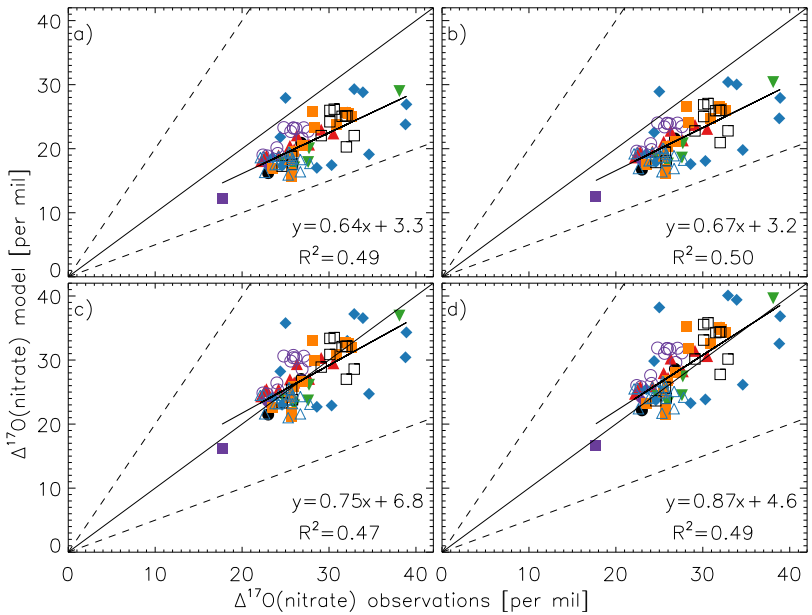

Fig. 2. Scatter plot of monthly-mean model calculations at the surface versus observations. Observations include: Bermuda (black circles), La Jolla (red triangles), South Pole (green triangles), DDU (blue diamonds), Chile (purple diamond), Princeton (purple open circles), Summit (orange squares), Alert (black open squares), Ecuador (purple square) and COCA (blue open triangles). Each panel uses different assumptions regarding the bulk isotopic composition of ozone and the isotopic transfer mechanism during ozone oxidation: **(a)** $\Delta^{17}O(O_3)$=35‰ and statistical $\Delta^{17}O$ transfer, **(b)** $\Delta^{17}O(O_3)$=25‰ and (Savarino et al., 2008) $\Delta^{17}O$ transfer applied to $NO+O_3$, **(c)** $\Delta^{17}O(O_3)$=35‰ and (Savarino et al., 2008) transfer applied to $NO+O_3$, **(d)** $\Delta^{17}O(O_3)$=35‰ and (Savarino et al., 2008) transfer applied to $NO+O_3$ and NO_2+O_3. The linear least-squares regression (thick), y=x (solid), y=2x and y=0.5x (dashed) lines are shown. Inset is the regression equation and R^2 values.

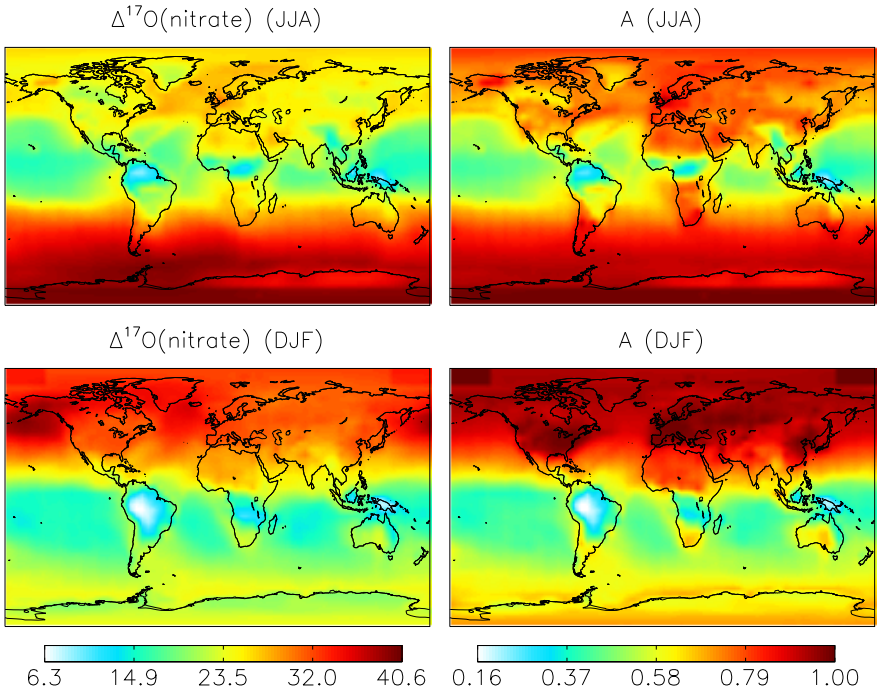

Fig. 3. Summer (JJA) (top) and winter (DJF) (bottom) average nitrate $\Delta^{17}O$ values (left) and *A*, the fraction of NO oxidized to NO_2 by O_3 (right) at the surface.

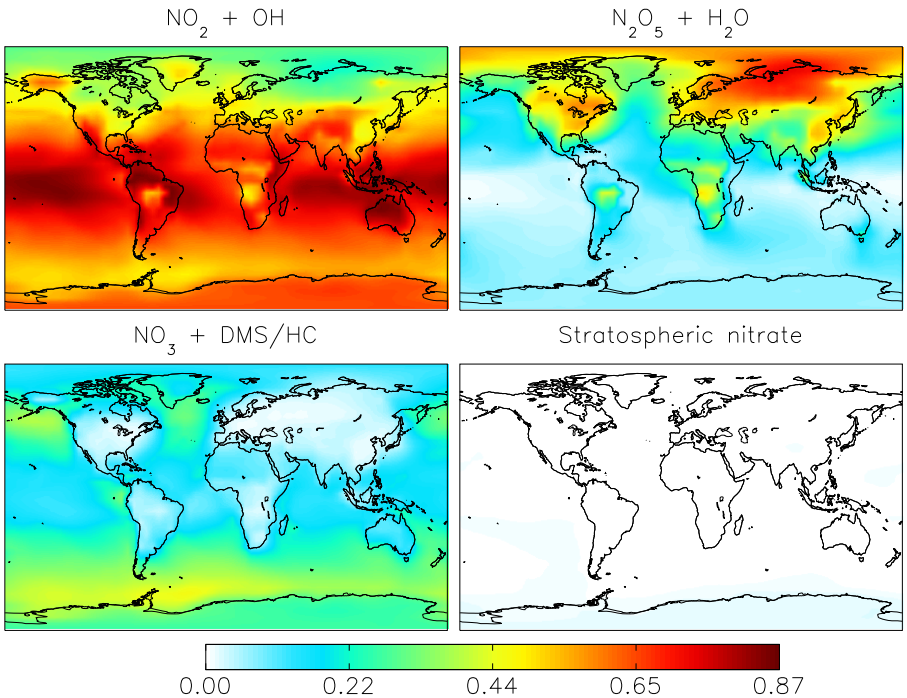

Fig. 4. Annual-mean fractional importance of each nitrate production pathway leading to total inorganic nitrate at the surface in the model: NO_2+OH (top left), N_2O_5 hydrolysis (top right), NO_3+DMS/HC (bottom left), and stratospheric nitrate (bottom right).

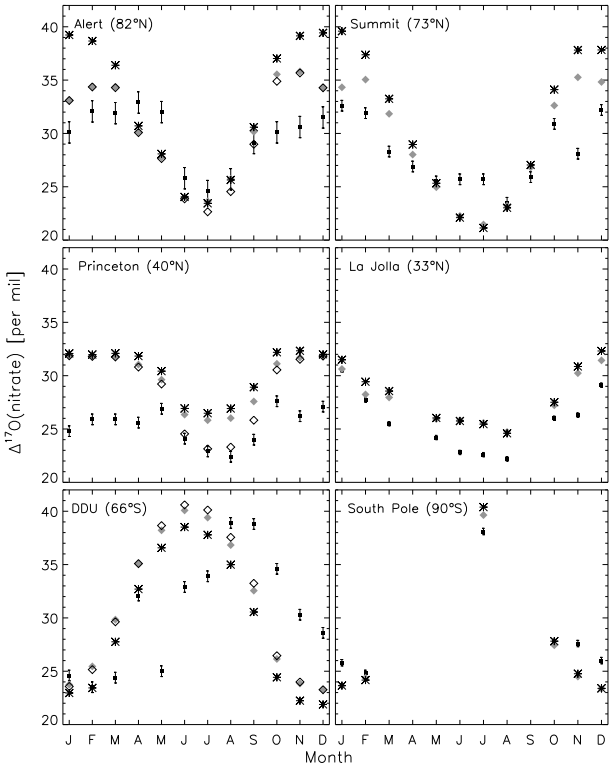

Fig. 5. Monthly mean nitrate $\Delta^{17}O$ (‰) observations (black squares with $\pm 1\sigma$ error bars) and model calculations at the surface (gray diamonds) at Summit, Greenland (Kunasek et al., 2008), Alert, Canada (Morin et al., 2008), Princeton, NJ (Kaiser et al., 2007), La Jolla, CA (Michalski et al., 2003), Dumont d'Urville, Antarctica (Savarino et al., 2007), and the South Pole (McCabe et al., 2007). Sensitivity simulation setting $\gamma_{N_2O_5}=0$ (asterisk) and simulation including organic nitrates in the $\Delta^{17}O$(nitrate) calculation (open diamonds) are also shown. The observations utilize the denitrifier method (Kaiser et al., 2007) (left panels) and the silver salt pyrolysis method (Michalski et al., 2002) (right panels).